ELSEVIER

Journal of Alloys and Compounds 330–332 (2002) 866–870

Journal of ALLOYS AND COMPOUNDS

www.elsevier.com/locate/jallcom

Influence of the boron additive on the electrochemical properties of the $MmNi_{3.55}Co_{0.75}Mn_{0.4}Al_{0.3}$ hydrogen storage alloy

H. Ye*, Y.X. Huang, T.S. Huang, H. Zhang

Division of Energy Science and Technology, Shanghai Institute of Metallurgy, CAS, 865 Changing Road, Shanghai 200050, PR China

Abstract

The $MmNi_{3.55}Co_{0.75}Mn_{0.4}Al_{0.3}B_x$ hydrogen storage alloys with various boron contents of $x=0$, 0.05, 0.1, 0.2, 0.3 were prepared by a radio frequency levitation melting process. The electrochemical kinetics such as linear polarization, electrochemical impedance spectroscopy and anodic polarization were investigated. Such experimental results showed that the addition of boron could enhance the activation performance and the rate capability. With the increase of boron additive such a favorable effect became more pronounced.

Keywords: Hydrogen storage materials; Electrochemical performance; High rate capability; Electrochemical impedance spectroscopy

1. Introduction

The nickel-metal hydride (Ni/MH) rechargeable battery shows good prospect in the field of high power applications such as cordless tools and electric vehicles. To meet this need, the development of the hydrogen storage alloy with superior rate capability is critical. Multi-component alloying is one of the most effective techniques to tailor properties so as to meet the application requirement of batteries [1–3]. Some studies [4–7] showed that by deviating AB_5-type compound composition from a stoichiometric ratio to non-stoichiometry could lead to better electrochemical performances. The deviation of stoichiometry and/or addition of other elements could change microstructure characteristics [4,5], thermodynamic and kinetic properties of hydrogen storage alloys [6,7]. Tadokoro et al. [8] have reported that the addition of boron into AB_5-type hydrogen-storage alloys could enhance their electrochemical reactivity. The improved electrochemical activity was ascribed to the presence of $MmCo_4B$ secondary phase. However, such a beneficial effect by the addition of the boron on the electrochemical properties of hydrogen storage alloys is not well understood.

The objective of this work was to systematically study the influence of the boron additive on the electrochemical properties of the commercial $MmNi_{3.55}Co_{0.75}Mn_{0.4}Al_{0.3}$ hydrogen storage alloy.

2. Experimental

The non-stoichiometric $MmNi_{3.55}Co_{0.75}Mn_{0.4}Al_{0.3}B_x$ hydrogen storage alloys with various boron contents of $x=0$, 0.05, 0.1, 0.2, 0.3 (hereafter noted as S_0, B_1, B_2, B_3, and B_4, respectively) were prepared by a radio frequency levitation melting processing in a copper crucible under an argon atmosphere using Mm (lanthanum-rich misch-metal containing 61.7% La, 27.4% Ce, 2.5% Pr and 8.4% Nd), nickel, cobalt, manganese, aluminum and boron with purities better than 99.5% as initial materials. The ingots were re-melted three times to ensure homogeneity, and then were annealed at 950°C for 6 h under Ar atmosphere. The ICP (inductively coupled plasma spectroscopy) analyzing results showed that the composition of prepared alloys is well consistent with the designed one. Then the as-prepared alloys were mechanically pulverized into powder. The powder with particle size ranges from 38 to 75 μm were used for the electrochemical measurements.

The preparation of electrodes and the setup of the trielectrode cell for electrochemical measurements have been described previously [7]. All electrochemical measurements were carried out at 20°C. The discharge capacity

*Corresponding author. Tel.: +86-216-251-1070x8803; fax: +86-216-225-4273.

E-mail address: yeqhui@itsvr.sim.ac.cn (H. Ye).

0925-8388/02/$ – see front matter
PII: S0925-8388(01)01484-0

of the electrode was determined by the galvanostatic method. The cutoff voltage for discharging was fixed at −0.6 V vs. Hg/HgO electrode. To evaluate the rate capability, the discharge capacity of electrode at different discharge current was measured. The cutoff voltages for different discharge current densities of 60, 300, 900, 1500 and 3000 mA g^{-1} were set to −0.6, −0.6, −0.5, −0.4, and −0.3 V vs. Hg/HgO electrode, respectively. Linear polarization (LP) was conducted at 50% depth of discharge (DOD) with the scanning rate of 1 mV s^{-1}. Anodic polarization (AP) was measured with the potential sweep rate from 25 to 0.5 mV s^{-1} beginning at 50% DOD. Electrochemical impedance spectroscopy (EIS) was obtained in the frequency range of 100 KHz to 1 mHz, with a.c. amplitude of 5 mV and the electrodes were maintained at the open-circuit state (50% DOD). High-rate capability, LP, AP and EIS were carried out with Solartron SI1287 Electrochemical Interface connected with a 1255B Frequency Response Analyzer after the investigated electrodes being completely activated (40 cycles).

3. Results and discussion

3.1. Activation performance and discharge capacity

Fig. 1 shows the activation profiles of the $MmNi_{3.55}Co_{0.75}Mn_{0.40}Al_{0.30}B_x$ electrodes. The activation was conducted under 60 mA g^{-1} current density. It is seen that the activation of $MmNi_{3.55}Co_{0.75}Mn_{0.40}Al_{0.30}$ was facilitated by the addition of boron. The S_0 electrode needs 10 cycles to reach its maximum discharge capacity, and only 2~3 cycles are needed for the B_1, B_2, B_3 and B_4 electrodes. However, the addition of boron lowers discharge capacity. As the amount of boron addition increases, the discharge capacity decreases monotonously. The maximum discharge capacities of S_0, B_1 B_2, B_3 and B_4 are 333.9, 321.4, 304.7, 271.7, and 256.0 mA h g^{-1}, respectively.

3.2. High rate capability

Fig. 2 shows the high rate dischargeability of the $MmNi_{3.55}Co_{0.75}Mn_{0.40}Al_{0.30}B_x$ electrodes. The high rate dischargeability of electrodes are expressed as $(C_{y\text{mA g}^{-1}}/C_{60\text{ mA g}^{-1}})\times 100\%$, where $C_{y\text{mA g}^{-1}}$ represents the discharge capacity at the current density of y mA g^{-1}, $C_{60\text{ mA g}^{-1}}$ represents the discharge capacity at 60 mA g^{-1}. It is observed that alloys containing boron additive show better high rate capability than that of stoichiometric S_0 alloy. At a high discharge current (≥1500 mA g^{-1}), such a favorable effect of boron additive is more evident. The higher content of the boron, the better the high-rate capability of alloy is. For example, the high-rate dischargeability of B_4 is close to 60% under 3000 mA g^{-1} current.

3.3. Electrochemical kinetic characteristics

The electrochemical performances of a hydrogen storage alloy are generally determined by its microstructure, thermodynamic and kinetic characteristics under the application environment. In the present study, the electrochemical kinetics of $MmNi_{3.55}Co_{0.75}Mn_{0.40}Al_{0.30}B_x$ electrodes were evaluated using LP, AP and EIS experiments.

Fig. 3 gives the linear polarization curves of $MmNi_{3.55}Co_{0.75}Mn_{0.40}Al_{0.30}B_x$ electrodes at 50% DOD. It

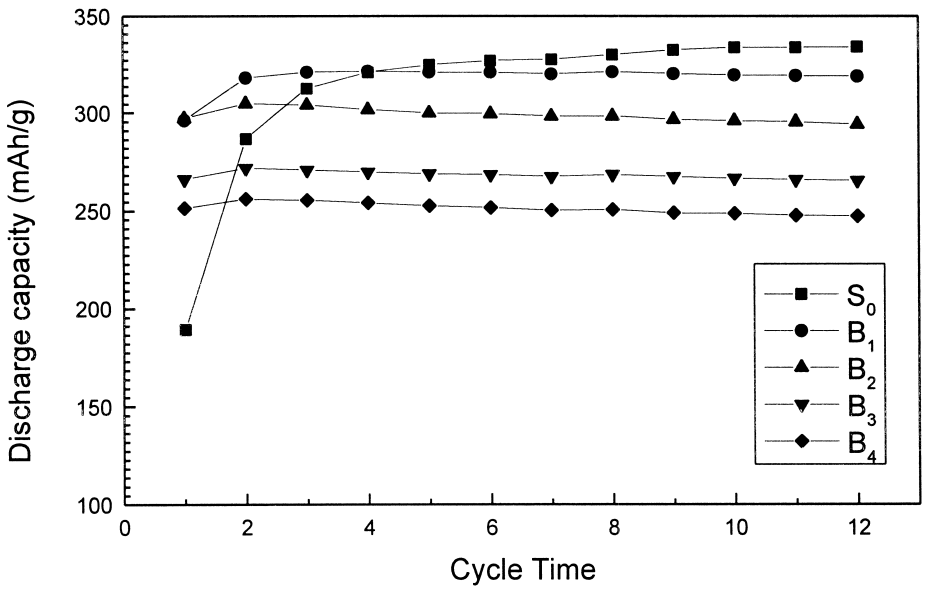

Fig. 1. Activation profiles of $MmNi_{3.55}Co_{0.75}Mn_{0.4}Al_{0.3}B_x$ electrodes.

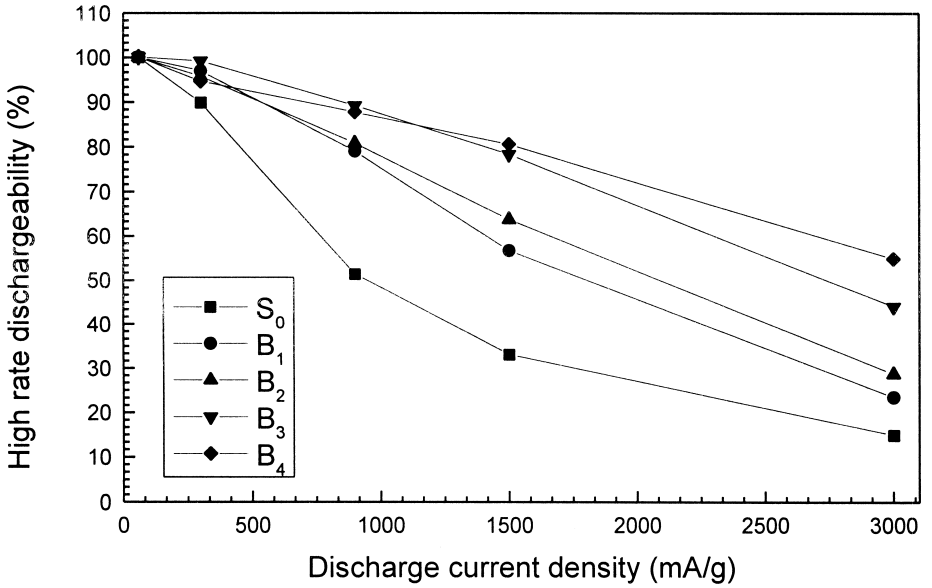

Fig. 2. Relationship between the high-rate dischargeability and the discharge current density of $MmNi_{3.55}Co_{0.75}Mn_{0.4}Al_{0.3}B_x$ electrodes.

is observed that the addition of boron lowers the polarization resistance of $MmNi_{3.55}Co_{0.75}Mn_{0.40}Al_{0.30}$ electrode. With the increase of boron content, the polarization resistances become even smaller. The exchange current densities I_0 for S_0, B_1, B_2, B_3 and B_4 determined from Fig. 3 are 356, 525, 551, 668 and 804 mA g^{-1}, respectively. This means that the addition of boron significantly increase the electrochemical activity of metal hydride electrode. Fig. 4 shows the EIS of $MmNi_{3.55}Co_{0.75}Mn_{0.40}Al_{0.30}B_x$ electrodes at 50% DOD. It is observed that all EIS consist of two semicircles followed by a straight line at low frequency. Using the analysis model proposed by Kuriyama et al. [9], the semicircle in the low-frequency region relates to the charge transfer reaction. The smaller diameter of this semicircle, the lower the charge transfer resistance, i.e. larger exchange current density of electrode would be. In the present case, with the increase of boron content (x from 0 to 0.3), the diameter of the second semicircle in the low frequency region decreases monotonously. This further confirms that the addition of boron improves the electrochemical activity of metal hydride electrode.

Typical anodic polarization curves of $MmNi_{3.55}Co_{0.75}Mn_{0.4}Al_{0.3}$ electrode at various potential sweep rates are shown in Fig. 5. With the increase of anodic overpotential, the polarization current increases

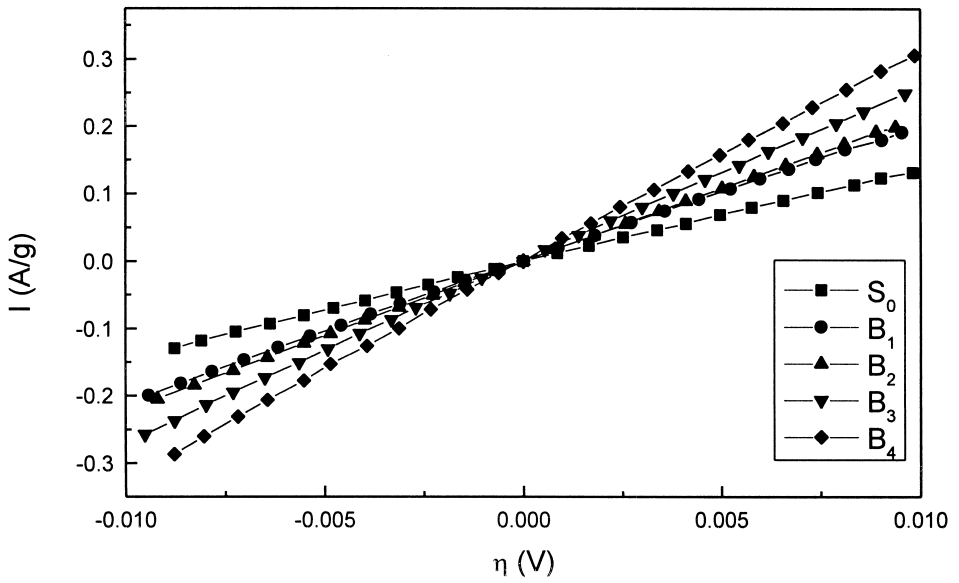

Fig. 3. Linear polarization curves of $MmNi_{3.55}Co_{0.75}Mn_{0.4}Al_{0.3}B_x$ electrodes obtained at 50% depth of discharge with the potential sweep rate of 1 mV s^{-1}.

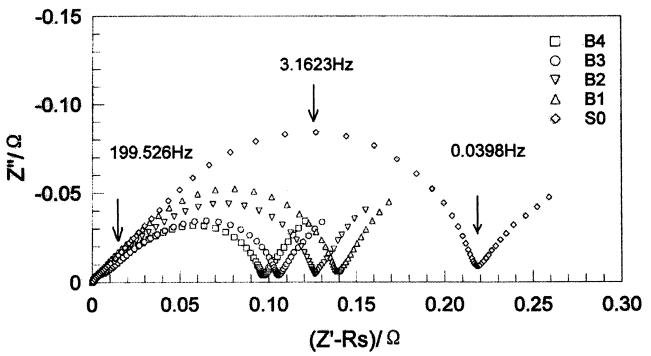

Fig. 4. Impedance spectra of the $MmNi_{3.55}Co_{0.75}Mn_{0.4}Al_{0.3}B_x$ electrodes measured at the 50% depth of discharge.

firstly to a maximum value then decreases gradually due to the oxidation of absorbed hydrogen. The peak current (I_P) is related to not only the rate of hydrogen diffusion in the alloy but also the electrocatalytic activity for hydrogen oxidation reaction [10]. From Fig. 5, it is observed that the I_P value increased with increasing potential sweep rate. Fig. 6 presents the I_p value as a function of square root of potential sweep rate ($\nu^{1/2}$) for $MmNi_{3.55}Co_{0.75}Mn_{0.4}Al_{0.3}B_x$ electrodes. It clearly shows that the I_P increases with the amount boron when potential sweep rate is higher than 1 mV s^{-1}, which indicates boron has favorable effect on kinetic properties of the electrode. The complex relation between I_P and boron content (x) at slow sweep rate ($\leq$1 mV s^{-1}) is because the capacity loss for B_1, B_2, B_3 and B_4 electrode during anodic polarization is considerable comparing with the initial capacity of investigated electrode (50% DOD) and the electrode with higher boron content itself has less capacity. Furthermore, the plot of I_p vs. $\nu^{1/2}$ for each investigated electrode in Fig. 6 gives a straight line but not passing through the origin in all cases. This is somewhat different from literature [10,11]. Inoue [10] and Geng et al. [11] reported that the plot of I_p vs. $\nu^{1/2}$ is a straight line and passing through the origin, indicating that the oxidation of absorbed hydrogen in the metal hydride electrode is controlled by the rate of hydrogen diffusion in the bulk of alloys and the slope of the straight line is proportional to the square root of hydrogen diffusion coefficient. In the present case, the straight lines not passing through the origin may be due to the different electrode-preparation technique and needs to be further studied. The slope of the straight line for $MmNi_{3.55}Co_{0.75}Mn_{0.4}Al_{0.3}B_x$ electrode in Fig. 6 is increased with the increase of boron content, also indicating that hydrogen diffusion in the alloys is facilitated by the addition of boron. This was confirmed by the constant-potential discharge results [12].

The XRD analysis shows that the stoichiometric S_0 compound without boron has single phase with $CaCu_5$-type, but all over-stoichiometric compounds with different boron content have a principal $CaCu_5$-type phase and a small amount of $CeCo_4B$-type phase, the amount of which increases with x increasing [12]. This is consistent with the results of Tadokoro et al. [8]. The boron is mainly in the secondary phase, which cannot hydride/dehydride reversibly thus impairs part of the electrochemical capacity [12]. The improved electrochemical activity of boron-containing alloys could be ascribed to the presence of $CeCo_4B$-type secondary phase [8,12]. However, the phase structure of our investigated boron-containing alloys is different from the results of Hu et al., who have reported that the as-cast AB_5-type alloys with small amounts of

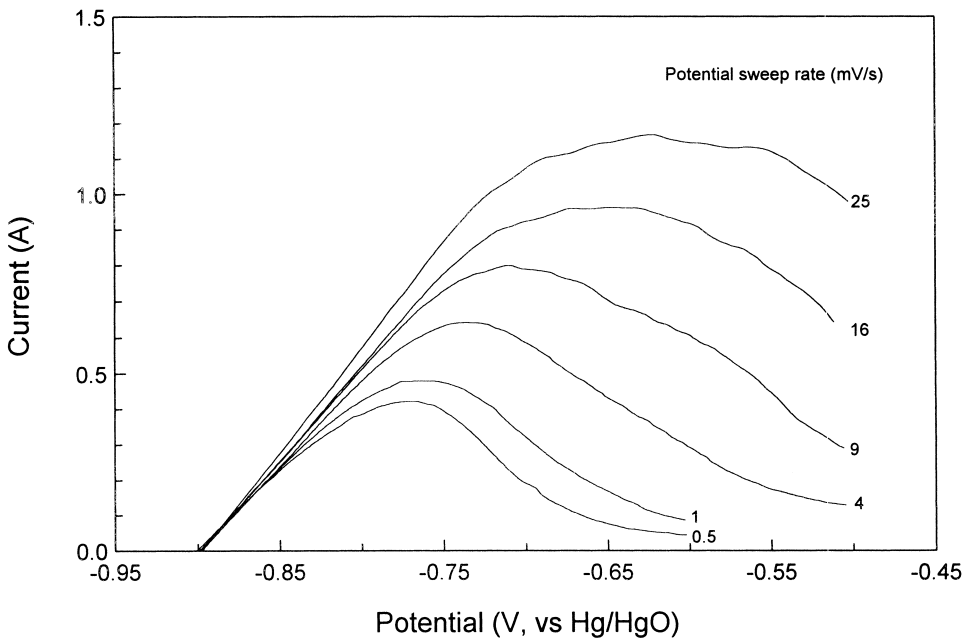

Fig. 5. Typical anodic polarization curves of $MmNi_{3.55}Co_{0.75}Mn_{0.4}Al_{0.3}$ electrode at various potential sweep rates measured at the 50% depth of discharge.

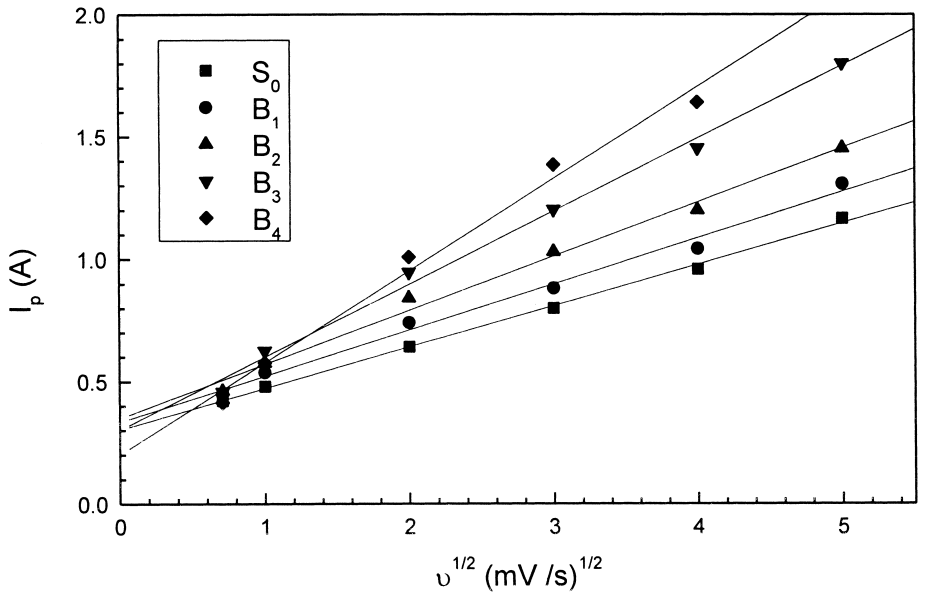

Fig. 6. Relationship between I_p and $\nu^{1/2}$ for $MmNi_{3.55}Co_{0.75}Mn_{0.4}Al_{0.3}B_x$ electrode.

boron having single phase $CaCu_5$-type structure [13]. The difference of phase structure of our investigated alloys may result from anneal treatment and the deviation to over-stoichiometry, both are of benefit for the formation of $CeCo_4B$-type secondary phase.

4. Conclusion

The electrochemical experimental results showed that the addition of boron enhanced the activation performance and rate capability of $MmNi_{3.55}Co_{0.75}Mn_{0.4}Al_{0.3}$ hydrogen storage alloy. These favorable effects became more significant with the increase of boron content. The unfavorable effect was that the addition of boron led to a decrease of electrochemical capacity at small current density. Linear polarization, electrochemical impedance spectroscopy and anodic polarization measurements revealed that the addition of boron improved the electrochemical activity at electrode surface and the hydrogen diffusion in the bulk of the alloy. The benefit of boron addition can be ascribed to the appearance of the secondary phase. The boron-containing over-stoichiometric hydrogen storage alloys are promising in some high power application fields of the Ni/MH battery.

References

[1] J.J.G. Willems, Philips J. Res. Suppl. 39 (1984) 1.
[2] H. Ogawa, M. Ikoma, H. Kawano, I. Matsumoto, in: T. Keily, B.W. Baxter (Eds.), Proceedings of the 16th International Power Sources Symposium, Bournemouth, 12 (1989) 393.
[3] T. Sakai, H. Yoshinaga, H. Migamura, N. Kuriyama, H. Ishikawa, J. Alloys Comp. 180 (1992) 37.
[4] P.H.L. Notten, P. Hokkeling, J. Electrochem. Soc. 138 (1991) 1877.
[5] C. Hong, Y. Zhang, J. Wang, J. Alloys Comp. 231 (1995) 546.
[6] Y. Fukumoto, M. Miyamoto, M. Matsuoka, C. Iwakura, Electrochim. Acta 40 (1996) 845.
[7] H. Ye, H. Zhang, J.X. Chen, T.S. Huang, J. Alloys Comp. 308 (2000) 163.
[8] M. Tadokoro, M. Nogami, Y. Chikano, M. Kimoto, T. Ise, K. Nishio, N. Fukukawa, J. Alloys Comp. 192 (1993) 179.
[9] N. Kuriyama, T. Sakai, H. Miyamura, I. Uehara, H. Ishikawa, J. Alloys Comp. 202 (1993) 183.
[10] H. Inoue, M. Miyamoto, M. Matsuoka, Y. Fukumoto, C. Iwakura, Electrochim. Acta 42 (1997) 1087.
[11] M.M. Geng, J.W. Han, F. Feng, D.O. Northwood, J. Electrochem. Soc. 146 (1999) 3591.
[12] H. Ye, H. Zhang, W.Q. Wu, T.S. Huang, J. Alloys Comp. 312 (2000) 68–76.
[13] W.-K. Hu, Z. Ye, D. Noreus, J. Alloys Comp. 280 (1998) 314.